Int J Clin Exp Med 2017;10(8):11728-11738
www.ijcem.com /ISSN:1940-5901/IJCEM0054237

Original Article

Predict microvascular invasion in hepatocellular carcinoma by dynamic contrast-enhanced magnetic resonance imaging in patients with hepatitis B virus

Xiaoming Zhou[1], Gang Wang[1], Yuanxiang Gao[1], Lan Yu[1], Wei Li[1], Linlin Jiao[2], Zhiming Li[1]

[1]*Department of Radiology,* [2]*Interventional Medical Center, The Affiliated Hospital of Qingdao University, Qingdao, PR China*

Received March 30, 2017; Accepted July 9, 2017; Epub August 15, 2017; Published August 30, 2017

Abstract: Purpose: To evaluate diagnostic performance of dynamic contrast-enhanced magnetic resonance imaging (MRI) for predicting microvascular invasion (MVI) of hepatocellular carcinoma (HCC) in patients with hepatitis B virus. Materials and Methods: This study was approved by our institutional review board, and the informed consent was waived. 107 patients accepted MR scanning before operation. Subsequently, 106 patients were performed liver mass resection, and one with liver transplantation. All images were evaluated by two radiologists with at least 9 years experience in abdominal MR imaging. The imaging features of tumors were as follows: peritumoral arterial enhancement, tumor pseudo-capsule, tumor margins, as well as multifocality. MVI, tumor size, Edmondson-Steiner grade and liver cirrhosis were also included. The independent Student's *t*-test was used to compare continuous variables, and the chi-squared test and Fisher's Exact test was used to analyze the categorical variables. Parameters shown to be statistically significant in univariate analysis were entered into a logistic regression model to identify independent predictors of MVI. The sensitivity, specificity, positive predictive value (PPV), and negative predictive value (NPV) were calculated. A *p*-value less than 0.05 was considered to be statistically significant. Results: By histopathologic analysis, 31.8% (34/107) of the patients with HCC were confirmed as MVI-positive, and 68.2% (73/107) were as MVI-negative. MVI was present in 11.8% (4/34) of tumors less than 5 cm with smooth margins; and 68.4% (13/19) of tumors larger than 5 cm with non-smooth margins. A larger (> 5 cm) tumor size (odds ratio [OR] 4.77, 95% CI 1.50-15.17; P < 0.05) and a non-smooth MRI tumor margin (OR 3.79, 95% CI 1.07-13.43; P < 0.05) were shown as independent predictors of MVI. The sensitivity, specificity, PPV, and NPV for predicting MVI by tumor size > 5 cm were 41.2% (95% CI 25.1-59.2), 86.3% (95% CI 75.8-92.9), 58.3% (95% CI 36.9-77.2), and 75.9% (95% CI 65.0-84.3), respectively. The sensitivity, specificity, PPV, and NPV for predicting MVI by a non-smooth margin were 87.1% (95% CI 69.2-95.8), 48.6% (95% CI 36.6-60.7), 42.9% (95% CI 30.7-55.9), and 89.5% (95% CI 74.3-96.6), respectively. When combining the tumor size (> 5 cm) with tumor margin (non-smooth margin) as the risk factors, the area under ROC curve was 0.732 (95% CI 0.624-0.840), and the OR value was 4.11 (95% CI 1.99-8.48; P < 0.05) for predicting presence of MVI. Conclusion: a non-smooth tumor margin and a larger tumor size could independently predict the presence of MVI. A tumor size > 5 cm and a non-smooth tumor margin could be used as preoperative predictors of the presence of MVI in patients with HCC.

Keywords: Hepatocellular carcinoma, magnetic resonance imaging, microvascular invasion

Introduction

Primary liver cancer is the sixth most common cancer and the second most common cause of cancer mortality worldwide [1]. Hepatocellular carcinoma (HCC) is the most frequently encountered primary liver cancer, accounting for 85%-90% of cases [2]. HCC in China accounts for 55% of all cases of HCC in the world, and the mortality associated with the disease has also increased worldwide [3, 4]. Major risk factors for HCC include hepatitis B virus (HBV) infection, hepatitis C virus (HCV) infection, alcoholic liver disease, and aflatoxin [3]. Although the effects of these factors on HCC are not entirely clear and the incidence of the disease varies in different regions worldwide because of different risk factors, HBV infection remains a major risk factor for development of HCC in China [4].

Vascular invasion, both macrovascular and microvascular, is considered to be a predictor of recurrence and poor likelihood of survival after hepatic resection and liver transplantation [5]. Macrovascular invasion and microvascular invasion (MVI) of HCC are related, respectively, to a 15-fold and 4.4-fold risk of tumor recurrence [6]. Macrovascular invasion is defined as invasion of a tumor into a major vessel and is easily identified on macroscopic examination or radiologic imaging. MVI is suggested by certain features, such as the presence of tumor emboli in a portal venous radicle, a large capsule vessel, or a vascular space lined by endothelial cells [7]. In contrast with macrovascular invasion, MVI is difficult to detect preoperatively using imaging techniques such as computed tomography (CT) or magnetic resonance imaging (MRI), and can only be confirmed by histopathologic examination. Preoperative methods for detecting the presence or absence of MVI could provide a choice of methods for predicting the outcome of hepatic resection or liver transplantation. Many studies have attempted to detect MVI preoperatively using radiologic imaging and specific laboratory tests [7-9]. Some radiologic studies have showed that MVI is closely related to a number of factors, including tumor size, number, margin, histologic grade, and gross classification of HCC [5]. However, there is still controversy regarding the value of these imaging features for identifying MVI. The aim of this study was to assess the accuracy of features seen on imaging for prediction of MVI in patients with HCC and HBV infection.

Materials and methods

Patients

This single-center retrospective study was approved by our institutional review board, and the requirement for informed consent was waived. Patients were identified by searching the electronic HIS database at the Affiliated Hospital of Qingdao University between June 2015 and July 2016. The study inclusion criteria were as follows: HBV infection; preoperative dynamic contrast-enhanced MRI performed in our radiology unit; an imaging diagnosis of HCC made on the basis of dynamic MRI evidence of a solitary hepatic tumor showing hypervascular enhancement in the arterial phase and contrast washout in the equilibrium phase [10]; no history of malignancy; agreement to undergo surgical resection or a liver transplant; and histopathology demonstrating HCC after hepatic resection or liver transplantation.

The exclusion criteria were as follows: previous locoregional treatment, such as transcatheter arterial chemoembolization, radiofrequency ablation, or hepatic resection; histopathology demonstrating cholangiocarcinoma; macrovascular invasion demonstrated on imaging or pathology; and MR images unsuitable for analysis because of motivation artifact. One patient with HCC and a polycystic liver was excluded because the border of the tumor was not defined well enough for accurate evaluation.

176 patients were identified via a search of clinical database management system. 35 of these received locoregional treatment, 8 patients histopathology demonstrated cholangiocarcinoma, 21 patients were confirmed with macrovascular invasion by MR imaging or pathologic analysis, and five patients' MR images failed to be evaluated. Therefore, the final study cohort comprised 107 patients (90 men, 17 women), with mean age of 56-year old (24-80; median 58). 106 patients accepted hepatic resection, while one patient accepted liver transplantation.

Image acquisition

MRI was performed on average 7 (range 1-23) days before surgery. All MR images were acquired on a 3.0 T MR unit (Signa HDxt; GE Medical Systems, Milwaukee, WI, USA) using an eight-channel, torso-phased-array coil centered over the liver.

The MR imaging included the following sequences: breath-hold, T2-weighted, single-shot, fast spin echo (TR/TE 1000-2000 ms/68 ms, matrix 288 × 224, slice thickness 5.0 mm, slice spacing 2 mm, field of view [FOV] 38 cm); respiratory-triggered, T2-weighted, fast spin echo (TR/TE 4000-8000 ms/81 ms, matrix 320 × 224, slice thickness 6.0 mm, slice spacing 2 mm, FOV 38 cm); diffusion-weighted imaging (b-value, 0 & 800 seconds/mm^2); and breath-hold, T1-weighted spoiled gradient recalled echo (TR/TE 4.06 ms/1.2 ms, matrix 256 × 180, slice thickness 5 mm, slice spacing 2.5 mm, FOV 38 cm).

Dynamic imaging, including the arterial phase, portal-venous phase, and equilibrium phase, was performed using the liver acquisition with volume acceleration sequence (TR/TE 2.55 ms/1.16 ms, matrix 256 × 224, slice thickness 6 mm, slice spacing 3 mm, FOV 38 mm) following administration of a dynamic injection of 20 mL of gadopentetate dimeglumine (Magnevist, Bayer Healthcare, Leverkusen, Germany) followed by a 20 mL saline flush at a rate of 2 mL/s using a contrast media injector.

Image analysis

All MR images were retrieved from the Picture Archiving and Communication System (Centricity PACS Radiology RA1000 Workstation, General Electric, Milwaukee, WI, USA) at our institution. The images were assessed by a consensus reading of two radiologists with 9 years (GW) and 10 years (YXG) experience in abdominal imaging. The two observers were aware only that the patients had HCC, and were blinded to any clinical and pathologic information. They analyzed the tumor imaging characteristics as follows: peritumoral arterial enhancement, tumor capsule, tumor margins, and multifocality of the lesions. In cases of multifocality, the largest lesion was included in the analysis. If there was a discrepancy between the two observers with regard to definition of tumor characteristics, the final decision was made by a third radiologist with 16 years of experience (XMZ).

The tumor capsule was defined as a hypointense thin linear structure encasing the tumor on arterial phase images and hyperintense on equilibrium phase images. We categorized the tumor capsule according to whether it was: complete (a capsule that completely surrounded the circumference of the tumor in the transverse and coronal planes); incomplete (a capsule that partially surrounded the circumference of the tumor); or absent (no capsule could be identified).

Peritumoral arterial enhancement was defined as the presence of a hyperintense, wedged, or irregular enhanced shape adjacent to the tumor on arterial phase that became isointense when compared with the normal liver parenchyma on equilibrium phase. We categorized peritumoral enhancement as either absent or present.

Tumor margins were defined as the interface between the tumor seen on MR images and the normal liver parenchyma. The tumor was assessed on T2-weighted images and on axial and coronal images in the equilibrium phase. We categorized each tumor as: single nodular type (a single nodular lesion with a smooth tumor-normal parenchyma interface on all images assessed); focal extranodular type (a focal outgrowth from the main nodular lesion, protruding into the normal parenchyma); and confluent multinodular or infiltrative type (tumor formed by a cluster of contiguous nodules or tumor with an entirely obscure tumor-normal parenchyma margin). We categorized the single nodular type as having a smooth tumor margin, and the focal extranodular and confluent multinodular or infiltrative types as having a non-smooth tumor margin.

Preoperatively, it was difficult to determine if multifocality indicated multicentric tumors or metastases for the main tumor, and intrahepatic metastasis could be caused by intravascular invasion or satellite micronodules from the tumor [11, 12]. Moreover, small tumor nodules were difficult to identify on preoperative radiology images alone. Therefore, we defined multifocality as being present when multiple lesions were identified on MRI or pathologic examination regardless of whether they were multicentric or metastatic tumors.

Pathologic analysis

All the HCC cases were confirmed by pathologic examination. Hepatic gross specimens were cut into slices 5 mm thick, fixed in 10% buffered formaldehyde solution, and paraffinized. The hematoxylin-eosin staining and immunohistochemistry analysis were performed by pathologists. The presence or absence of MVI was described by our institutional pathologic reports and all pathologic examinations were performed by a team of pathologists who were blinded to the MRI findings. The degree of tumor differentiation was categorized according to the Edmondson-Steiner nuclear grading system [13]; when different grades were found within the same tumor, the predominant grade was recorded. MVI was defined as a tumor within a vascular space lined by endothelium that was visible only on microscopy [14]. The tumor size, Edmondson-Steiner grade, MVI, and multi-

Table 1. Clinical and histopathologic characteristics of 107 patients with hepatocellular carcinoma

Clinical and histopathologic characteristics	All patients (n = 107)	MVI-negative (n = 73)	MVI-positive (n = 34)	*P*-value
Age, years (mean ± SD)	56.50 ± 10.30	56.41 ± 10.23	56.71 ± 10.62	0.891
Sex (Male/Female)	90/17	60/13	30/4	0.426
Presence of cirrhosis (Yes/No)	53/54	35/38	18/16	0.63
Histologic grade (I/II/III)	4/55/48	4/41/38	0/14/20	0.075

Abbreviation: MVI, microvascular invasion.

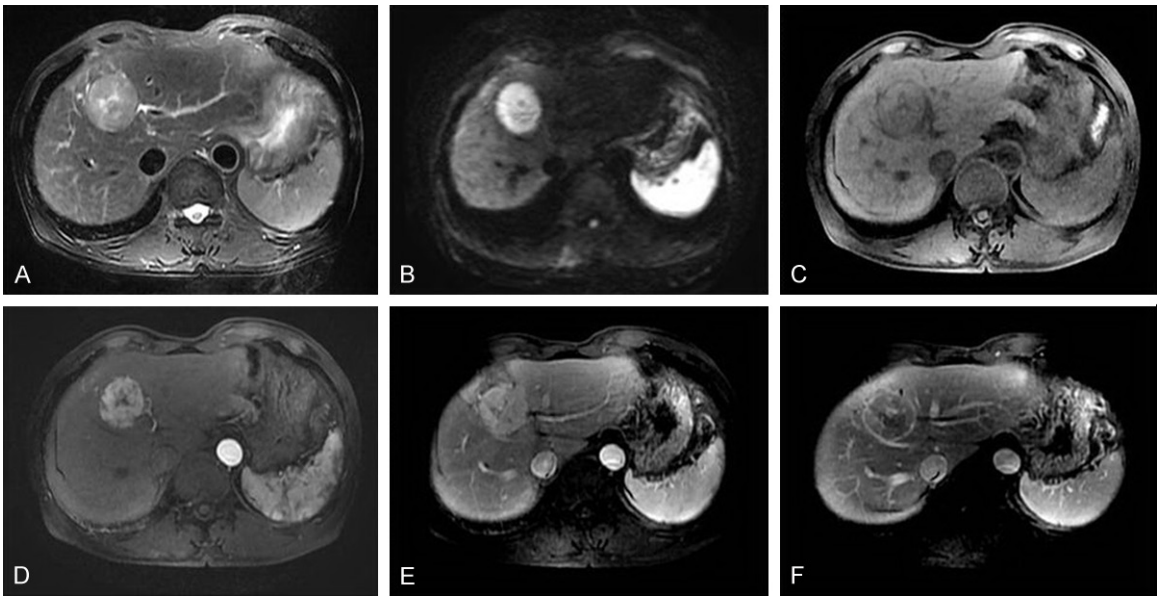

Figure 1. A solitary hepatocellular carcinoma of the single nodular type in a 67-year-old man confirmed as MVI-negative by pathologic analysis. A T2-weighted image (A) and a diffusion-weighted image (B) show hyperintensity. A T1-weighted image (C) shows a hypointense tumor in segment IV. T1-weighted images at arterial phase (D), portal-venous phase (E), and equilibrium phase (F) show an arterial phase enhancing tumor and washout on equilibrium phase. A coronal image also shows a smooth tumor-normal parenchyma interface. Abbreviation: MVI, microvascular invasion.

focality of the tumor were recorded. The presence of cirrhosis was also documented.

Statistical analysis

The independent Student's *t*-test was used to compare continuous variables (patient age, tumor size) between the MVI-positive and MVI-negative groups. The chi-squared test and Fisher's Exact test was used to analyze the categorical variables, including patient sex, presence of cirrhosis, Edmondson-Steiner grade, tumor margins, radiologic tumor capsule, peritumoral arterial enhancement, and multifocality of the lesions. Parameters shown to be statistically significant in univariate analysis were entered into a logistic regression model to identify independent predictors of MVI. The area under the receiver operating characteristic (ROC) curve was used to determine the cutoff-value of tumor size, and predict the diagnostic performance of two risk factors (tumor size > 5 cm, and non-smooth tumor margin) for evaluating MVI. The sensitivity, specificity, positive predictive value (PPV), and negative predictive value (NPV) were calculated for the parameters found to be statistically significant in multivariate analysis. A *P*-value < 0.05 was considered to be statistically significant. All statistical analyses were performed using Statistical Package for Social Science version 17.0 software (SPSS Inc., Chicago, IL, USA).

Results

One hundred and seven HCC tumors were included in the study. All patients had HBV infection confirmed by serum testing and two

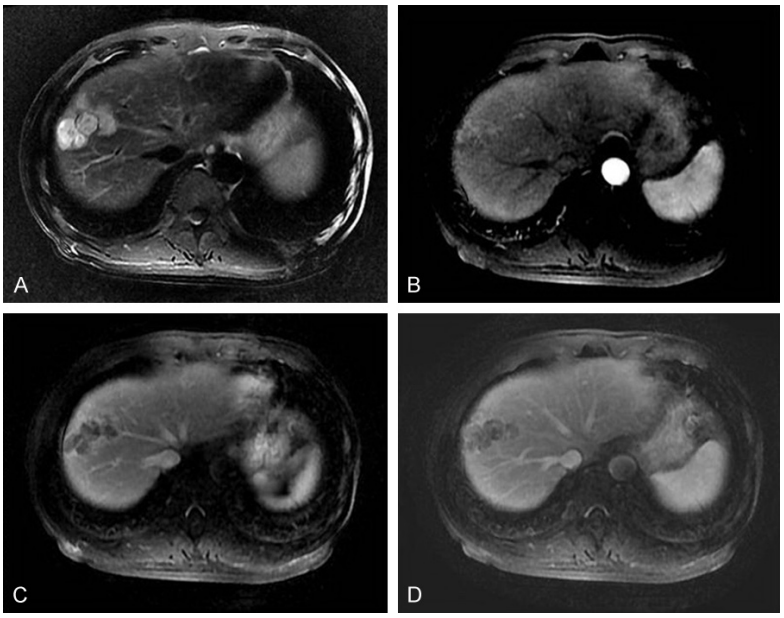

Figure 2. A confluent hepatocellular carcinoma of the multinodular type in a 56-year old man confirmed as MVI-positive by pathologic analysis. A T2-weighted image (A) shows a hyperintense tumor formed by a cluster of contiguous nodules. T1-weighted images at arterial phase (B), portal-venous phase (C), and equilibrium phase (D) show arterial phase enhancing and washout on portal-venous phase and equilibrium phase. Abbreviation: MVI, microvascular invasion.

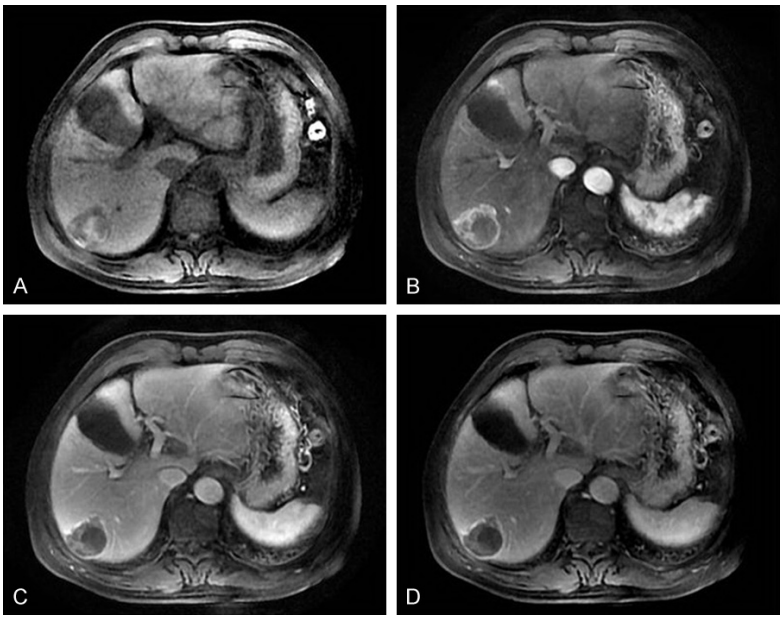

Figure 3. A hepatocellular carcinoma of the focal extranodular type in a 61-year old man confirmed to be MVI-positive by pathologic analysis. A T1-weighted image (A) shows a hyperintense area in the hypointense tumor (confirmed necrosis and hemorrhage on pathologic analysis). T1-weighted images at arterial phase (B), portal-venous phase (C), and equilibrium phase (D) show arterial phase enhancing and washout on portal-venous phase and equilibrium phase and focal outgrowth from the main nodular lesion, protruding into the normal parenchyma.

had both HBV and HCV infection. In one patient, segment VI of the tumor had invaded the right adrenal gland and another patient had bone metastases. None of the patients had lymph node metastasis. The clinical characteristics of the patients and their histopathologic findings are shown in **Table 1**.

MVI from histological findings

Histopathologic analysis revealed that 31.8% (34/107) of the patients with HCC were MVI-positive and 68.2% (73/107) were MVI-negative. All patients included in our study were divided into two groups: MVI-positive group, and MVI-negative group.

MRI findings

Tumor size: The mean size for all the HCC tumors was 4.22 ± 2.21 cm. The tumor size was 3.68 ± 1.55 cm in the MVI-negative group, and 5.41 ± 2.87 cm in the MVI-positive group.

Peritumoral arterial enhancement and tumor capsule

Peritumoral arterial enhancement was present in 21.5% of lesions (23/107), and the radiologic tumor capsule was incomplete in 62.6% (67/107) and complete in 27.1% (29/107), respectively.

Tumor margin

Six patients had tumors that became isointense in equilibrium phase, so it was difficult to identify the interface between the tumor and the

Table 2. Univariate analysis of MRI findings with and without MVI in patients with hepatocellular arcinoma

MRI characteristics	Patients (n = 107)	MVI-negative (n = 73)	MVI-positive (n = 34)	*p*-value
Peritumoral arterial enhancement (Present/Absent)	23/84	14/59	9/25	0.393
Tumor capsule (Absent/Incomplete/Complete)	11/67/29	9/41/23	2/26/6	0.121
Tumor margin (Smooth/Non-smooth)	38/63*	34/36	4/27	0.001
Tumor size, cm (mean ± SD)	4.22 ± 2.21	3.68 ± 1.55	5.41 ± 2.87	< 0.001
Multifocality (Absent/Present)	82/25	59/14	23/11	0.134

*Six patients excluded for evaluation of tumor margin. Abbreviation: MRI, magnetic resonance imaging; MVI, microvascular invasion.

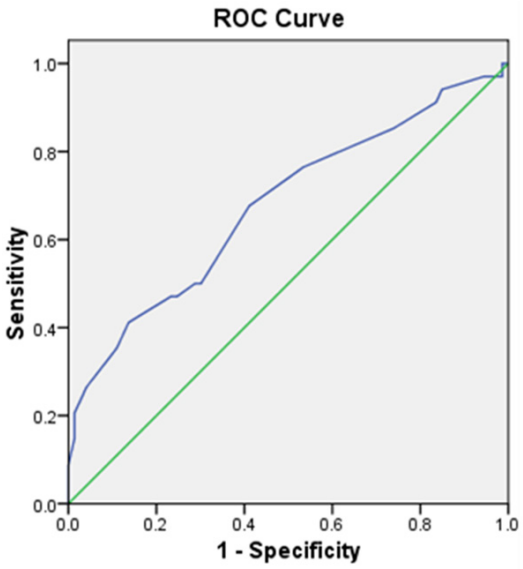

Figure 4. Area under the receiver-operating characteristic curve for tumor size with a cutoff value of 5 cm was 0.677 (P = 0.003, 95% confidence interval 0.56-0.791).

normal parenchyma. Therefore, evaluation of tumor margins on MRI was not possible in these patients. Of the 101 patients in whom tumor margins were evaluated, 37.6% (38/101) presented as the single nodular type, 18.8% (19/101) as the extranodular type, and 43.6% (44/101) as the multinodular or infiltrative type. Thirty-eight lesions had smooth tumor margins (**Figure 1**) and 63 had non-smooth margins on MRI (**Figures 2** and **3**). MVI was present in 11.8% (4/34) of tumors less than 5 cm with smooth margins; and 68.4% (13/19) of larger than 5 cm tumors with non-smooth margins.

Multifocality of HCC

On histologic examination, 25/107 of the patients (23.4%) had multifocal lesions, which were detected by MRI in 18 cases.

The MRI features are shown in **Table 2**.

Statistical results

There were no significant differences between the two groups with regard to age, sex, presence of cirrhosis, or Edmondson-Steiner grade.

There was a statistically significant association between tumor size and the presence of MVI (P < 0.05). Based on the area under the ROC curve for tumor size, the cutoff value of tumor size was 5 cm, the AUC was 0.677 (P < 0.05, 95% confidence interval [CI] 0.563-0.791) for predicting MVI (**Figure 4**). The sensitivity, specificity, PPV, and NPV for predicting MVI by tumor size > 5 cm were 41.2% (95% CI 25.1-59.2), 86.3% (95% CI 75.8-92.9), 58.3% (95% CI 36.9-77.2), and 75.9% (95% CI 65.0-84.3), respectively.

A statistically significant association was found between tumor margins and the presence of MVI (P < 0.05). In univariate analysis, the tumor margin had a statistically significant relationship with MVI (P < 0.05). The sensitivity, specificity, PPV, and NPV for predicting MVI from the non-smooth margin were 87.10% (95% CI 69.24-95.78), 48.57% (95% CI 36.57-60.73), 42.86% (95% CI 30.68-55.91), and 89.47% (95% CI 74.26-96.57), respectively.

In univariate analysis, there was no statistically significant difference in radiologic tumor capsule, peritumoral arterial enhancement, or multifocality of lesions between the MVI-negative group and the MVI-positive group.

To illustrate the relationship between histologic grade, tumor size or tumor margin and MVI, multivariate regression analysis was performed (**Table 3**). Both univariate analysis and multivariate logistic regression analysis showed that

Table 3. Multivariate logistic regression analysis of parameters predicting microvascular invasion

Characteristics	Beta value	OR	95% CI	*P*-value
MRI tumor margin	1.332	3.789	1.069-13.425	0.039
Size > 5 cm	1.562	4.767	1.498-15.171	0.008
Peritumoral arterial enhancement	-0.361	0.697	0.201-2.420	0.570
Tumor capsule	-0.189	0.828	0.328-1.087	0.689
Multifocality	0.153	1.165	0.337-4.030	0.809
Histologic grade	1.257	3.516	1.210-10.219	0.021
Gender	-1.087	0.337	0.064-1.764	0.198
Age	-0.012	0.989	0.940-1.040	0.653

Abbreviations: CI, confidence interval; MVI, microvascular invasion; OR, odds ratio.

Table 4. Combing the tumor size (> 5 cm) with tumor margin (non-smooth margin) together as the risk factors

Factors*	MVI-negative (n = 70)	MVI-positive (n = 31)	Percentage of MVI-positive (%)
0 risk factor	30	4	11.8
1 risk factor	34	14	29.3
2 risk factors	6	13	68.4

*Six patients excluded for evaluation of tumor margin and risk factors. Abbreviations: MVI, microvascular invasion.

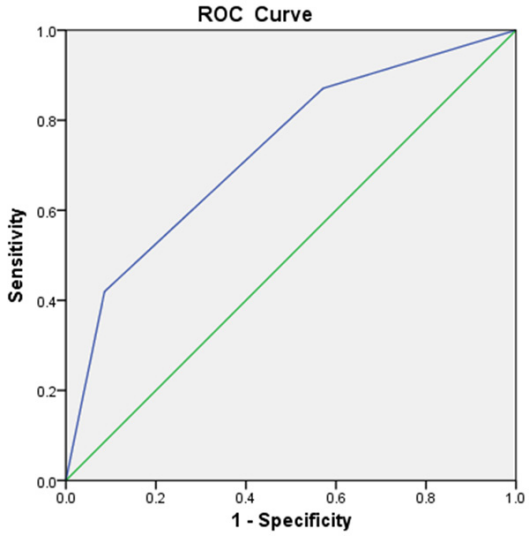

Figure 5. Area under the receiver-operating characteristic curve for two risk factor in predicting MVI. When combining the tumor size (> 5 cm) with tumor margin (non-smooth margin) together as the risk factors, ROC was used to analyze the risk factors for predicting MVI (shown in **Figure 5**), with the area under ROC of 0.732 (95% CI 0.624-0.840).

a larger (> 5 cm) tumor size (odds ratio [OR] 4.41, 95% CI 1.70-11.46; $P < 0.05$) and a non-smooth MRI tumor margin (OR 6.38, 95% CI 2.10-20.13; $P < 0.05$) were independent predictors of MVI.

When combining the tumor size (> 5 cm) with tumor margin (non-smooth margin) together as the risk factors (**Table 4**), ROC was used to analyze the risk factors for predicting MVI (shown in **Figure 5**), with the area under ROC of 0.732 (95% CI 0.624-0.840). The risk factors (odds ratio [OR] 4.11, 95% CI 1.99-8.48; P < 0.05) were associated with positive MVI.

Discussion

Recent studies suggest that MVI is a strong predictor of outcome in patients with HCC [15-17]. Therefore, identification of MVI preoperatively paves the way for new curative and palliative treatment options, including liver transplantation, hepatic resection, ablation, transarterial chemoembolization, and radioembolization. In MVI-positive patients, a more aggressive treatment strategy can be used, such as a larger ablation area in combination with transcatheter arterial chemoembolization or radioembolization [18]. In our study, we prospectively assessed clinical, pathologic, and MRI findings as predictors of MVI.

We measured the tumor size according to the pathology result. Tumor size was found to have a statistically significant correlation with the presence of MVI in several studies that used univariate analysis [19-22]. According to our results, a larger tumor size was significantly correlated with MVI in both univariate and multivariate analysis, as in other reports [18, 23]. Renzulli et al. [18] divided tumor size into three groups (< 2 cm, 2-5 cm, > 5 cm), and when tumor size was combined with other "worrisome" imaging features, it could predict MVI in HCC. However, the cutoffs for tumor size predicting the presence of MVI are controversial, being reported as ≥ 3 m in Hirokawa et al. [24], > 5 cm in Ahn et al. [25], and > 7 cm in Yasuhiko

et al. [23]. The Milan criteria are typically used for surgery, but adoption of expanded criteria is presently suggested by a number of centers because patients who do not meet the Milan criteria are excluded from potentially curative surgery. Thus, in our study, more patients (24/107) not meeting the Milan criteria were included. We grouped tumor size at a cutoff of > 5 cm for predicting MVI, and the sensitivity, specificity, PPV, and NPV values were 41.2% (95% CI 25.1-59.2), 86.3% (95% CI 75.8-92.9), 58.3% (95% CI 36.9-77.2), and 75.9% (95% CI 65.0-84.3), respectively.

Depending on their appearance on MRI, we categorized tumor margins into three groups, i.e., a focal extranodular type, a confluent multinodular type, or an infiltrative type if the tumor margin was non-smooth. Our findings suggest that a non-smooth tumor margin is significantly associated with the presence of MVI. Chou et al. [20] reported that a non-smooth tumor margin detected on multiphasic CT correlated with the histopathologic presence and location of MVI; in their study, the presence of a non-smooth tumor margin had a sensitivity of 81.7% (95% CI 71.9-91.5), a specificity of 88.1% (95% CI 78.3-97.9), an accuracy rate of 84.3% (95% CI 77.3-91.4), a PPV of 90.7% (95% CI 83.0-98.5), and an NPV of 77.1% (95% CI 65.2-91.4). Chou et al. [20] also indicated that MVI occurred most frequently at sites of extranodular extension. A number of other studies have also concluded that a non-smooth tumor margin can predict the presence of MVI [21, 26]. In our study, we found that the non-smooth margin seen on MRI had a sensitivity, specificity, PPV, and NPV of 87.10% (95% CI 69.24-95.78), 48.57% (95% CI 36.57-60.73), 42.86% (95% CI 30.68-55.91), and 89.47% (95% CI 74.26-96.57), respectively. The differences in specificity and PPV between our study and those reported by Chou et al. [20] may lie in patient selection bias, in that our study contained more MVI-negative patients. Another reason may be the different imaging sources used, in that we used MRI and Chou et al. used multidetector CT. The more recent MRI protocols have improved the visualization of tumor margins on hepatobiliary phase using gadolinium ethoxybenzyl-diethylenetriaminepentaacetic acid (Gd-EOB-DTPA)-enhanced MRI [26]. Ariizumi et al. [26] demonstrated that a non-smooth margin in the axial hepatobiliary phase was a significant predictor of both microscopic portal vein invasion (OR 18.814, $P = 0.024$) and intrahepatic metastasis (OR 6.498; $P = 0.036$) of HCC on multivariate analysis. In our study, a non-smooth margin was identified as a significant predictor of MVI (OR 6.38, 95% CI 2.10-20.13; $P < 0.05$). Differences in patient cohorts, study design, and the phases acquired using different MRI-enhanced contrast agents should also be taken into account. Further, Renzulli et al. [18] reported that larger tumor size, non-smooth tumor margins, peritumoral enhancement, and two-trait predictor of venous invasion were “worrisome” imaging features that could indicate MVI in patients with HCC. We found that MVI was present in 11.8% of cases with which had both features of smooth margin and less than 5 cm of tumor size; and 68.4% of cases with non-smooth margin and tumor size of larger than 5 cm. Thus, the presence of MVI was 6-fold higher in patients with a larger tumor size and non-smooth margins. Our findings indicate that a combination of larger tumor size and non-smooth tumor margins is a good predictor of the presence of MVI.

Radiologic peritumoral arterial enhancement has been reported to be suggestive of an increased risk of MVI [19, 27]. Miyata et al. observed that enhanced coronal distortion and a tumorous arterioportal shunt seen on CT hepatic arteriography could be significant predictors of a tumor that has invaded the portal vein. Kim et al. [19] also demonstrated that irregular circumferential peritumoral arterial enhancement could be a predictor of MVI. Our results in 23/107 patients indicated no significant relationship between the existence of peritumoral arterial enhancement and the presence of MVI. There are several possible reasons for the discrepancy between our study findings and those of Kim et al. [19]. In their study, Kim et al. obtained four arterial phase MRI scans at the same level and a significant difference with regard to prediction of MVI was only found in the third arterial phase, whereas in our study we acquired only one arterial phase that included the whole liver. Kim et al. showed that irregular enhancement rather than wedge-shaped enhancement was a risk factor for MVI. In our study, we defined peritumoral arterial enhancement as the existence of a hyperintense wedged or irregular-shaped appearance adjacent to the tumor on arterial phase. However,

we did not categorize our peritumoral arterial enhancement pattern as irregular or wedge-shaped. Nevertheless, our results are consistent with some of the other reports [20, 21]. Further studies of the relationship between peritumoral arterial enhancement and MVI are needed.

A surrounding fibrous capsule may accompany HCC in 10%-70% of cases [28]. Slow flow in the microvasculature of the capsule may be the reason for the late enhancement [29]. Adachi et al. [30] reported that blood vessels in the fibrous capsule were frequently invaded by cancer cells, and suggested that the presence of a fibrous capsule was a predictor of portal venous invasion. In contrast, Lim et al. [31] reported that the presence of a capsule on CT was significantly correlated with histopathology and that disruption of the capsule seen on CT was correlated with MVI. In other studies [32], the presence of a fibrous capsule in HCC has been shown to be a favorable prognostic factor because the capsule may prevent invasion of HCC into the adjacent liver parenchyma. The relationship between the presence or absence of a tumor capsule and MVI is controversial. In our study, we categorized the radiologic capsule into three groups, i.e., absent, incomplete, or complete, and found no relationship between any capsule group and the presence of MVI. Our results in this regard are similar to those of Kim et al. [19], Xu et al. [33], and Chandarana et al. [34].

Chandarana et al. [34] found that tumor multifocality was the only variable that was significantly correlated with the presence of MVI. They also reported that the presence of three or more tumors on MRI and four or more tumors on pathologic examination had high specificity (88.2% and 91.2%, respectively) for prediction of MVI. In our patients, 23.4% (25/107) had multifocal lesions verified by histologic examination, and these lesions had no significant correlation with MVI. The difference in findings between our study and that of Chandarana et al. may lie in a degree of selection bias and the different study designs used, in that their study cohort fulfilled the Milan criteria whereas our patients had small multifocal lesions.

HBV is a double-stranded virus containing DNA that is able to integrate its DNA into hepatic cells, act as a mutagenic agent, and cause secondary chromosomal rearrangement and increased genomic instability [35]. The burden of HCC is greatest (> 80%) in sub-Saharan Africa and Eastern Asia, where HBV infection is endemic. In contrast, HCV infection is more predominant in the USA, Europe, and Japan, so is the major risk factor for HCC in these regions [36]. Almost 50% of cases of HCC are associated with HBV and 25% are associated with HCV worldwide [35]. There was no evidence for the presence/absence of MVI in patients with HCC associated with HBV or any other condition known to be associated with HCC. Our study evaluated the correlation of clinical, pathologic, and MRI findings with MVI in HBV-infected patients, and no difference was found between our results and those of previous studies in patients with related conditions [34]. Moreover, there were two patients coinfected with HBV and HCV in our study.

Our study had several limitations. First, it was retrospective in nature and contained some selection bias arising from the fact that all the patients investigated were candidates for surgery. This may mean that our patients are not representative of the general patient population with HCC. Second, most of our patients were MVI-negative, which could be a further source of selection bias. Third, we did not undertake an independent analysis by multiple reviewers, so could not obtain interobserver agreement. Fourth, newer imaging methods, such as hepatobiliary phase Gd-EOB-DTPA-enhanced MRI, were not used in our study, and tumor margins were inadequate for evaluation in some patients. Images for 6 patients showed isointensity in equilibrium phase and had to be excluded from the evaluation of tumor margins on MRI.

In conclusion, our study suggests that a non-smooth tumor margin and a larger tumor size could independently predict the presence of MVI. A tumor size > 5 cm and a non-smooth tumor margin could be used as preoperative predictors of the presence of MVI in patients with HCC.

Disclosure of conflict of interest

None.

Address correspondence to: Dr. Zhiming Li, Department of Radiology, The Affiliated Hospital of Qingdao

University, Qingdao, PR China. E-mail: zhiminglee@yeah.net

References

[1] Ferlay J, Soerjomataram I, Dikshit R, Eser S, Mathers C, Rebelo M, Parkin DM, Forman D, Bray F. Cancer incidence and mortality worldwide: sources, methods and major patterns in GLOBOCAN 2012. Int J Cancer 2015; 136: E359-E386.

[2] El-Serag HB, Rudolph KL. Hepatocellular carcinoma: epidemiology and molecular carcinogenesis. Gastroenterology 2007; 132: 2557-2576.

[3] Stewart BW, Wild C. World cancer report 2014. World Health Organization: Lyon, France; 2014.

[4] Lyu X, Liu K, Chen Y, Wang Z, Yao J, Cai G, Jiang Z, Wang Z, Jiang J, Gu H. Analysis of risk factors associated with the development of hepatocellular carcinoma in chronic HBV-infected Chinese: a meta-analysis. Int J Environ Res Public Health 2016; 13.

[5] Unal E, Idilman IS, Akata D, Ozmen MN, Karcaaltincaba M. Microvascular invasion in hepatocellular carcinoma. Diagn Interv Radiol 2016; 22: 125-132.

[6] Iwatsuki S, Dvorchik I, Marsh JW, Madariaga JR, Carr B, Fung JJ, Starzl TE. Liver transplantation for hepatocellular carcinoma: a proposal of a prognostic scoring system. J Am Coll Surg 2000; 191: 389-394.

[7] Rodriguez-Peralvarez M, Luong TV, Andreana L, Meyer T, Dhillon AP, Burroughs AK. A systematic review of microvascular invasion in hepatocellular carcinoma: diagnostic and prognostic variability. Ann Surg Oncol 2013; 20: 325-339.

[8] Gouw AS, Balabaud C, Kusano H, Todo S, Ichida T, Kojiro M. Markers for microvascular invasion in hepatocellular carcinoma: where do we stand? Liver Transpl 2011; 17 Suppl 2: S72-S80.

[9] Yamashita Y, Shirabe K, Aishima S, Maehara Y. Predictors of microvascular invasion in hepatocellular carcinoma. Dig Dis 2015; 33: 655-660.

[10] Bruix J, Sherman M; American Association for The Study of Liver Diseases. Management of hepatocellular carcinoma: an update. Hepatology 2011; 53: 1020-1022.

[11] Kubo S, Nishiguchi S, Hirohashi K, Shuto T, Kuroki T, Minamitani S, Ikebe T, Yamamoto T, Wakasa K, Kinoshita H. Clinicopathological criteria for multicentricity of hepatocellular carcinoma and risk factors for such carcinogenesis. Jpn J Cancer Res 1998; 89: 419-426.

[12] Shi M, Zhang CQ, Zhang YQ, Liang XM, Li JQ. Micrometastases of solitary hepatocellular carcinoma and appropriate resection margin. World J Surg 2004; 28: 376-381.

[13] Edmondson HA, Steiner PE. Primary carcinoma of the liver: a study of 100 cases among 48,900 necropsies. Cancer 1954; 7: 462-503.

[14] Roayaie S, Blume IN, Thung SN, Guido M, Fiel MI, Hiotis S, Labow DM, Llovet JM, Schwartz ME. A system of classifying microvascular invasion to predict outcome after resection in patients with hepatocellular carcinoma. Gastroenterology 2009; 137: 850-855.

[15] Sumie S, Nakashima O, Okuda K, Kuromatsu R, Kawaguchi A, Nakano M, Satani M, Yamada S, Okamura S, Hori M, Kakuma T, Torimura T, Sata M. The significance of classifying microvascular invasion in patients with hepatocellular carcinoma. Ann Surg Oncol 2014; 21: 1002-1009.

[16] Lim KC, Chow PK, Allen JC, Chia GS, Lim M, Cheow PC, Chung AY, Ooi LL, Tan SB. Microvascular invasion is a better predictor of tumor recurrence and overall survival following surgical resection for hepatocellular carcinoma compared to the Milan criteria. Ann Surg 2011; 254: 108-113.

[17] Goh BK, Chow PK, Teo JY, Wong JS, Chan CY, Cheow PC, Chung AY, Ooi LL. Number of nodules, Child-Pugh status, margin positivity, and microvascular invasion, but not tumor size, are prognostic factors of survival after liver resection for multifocal hepatocellular carcinoma. J Gastrointest Surg 2014; 18: 1477-1485.

[18] Renzulli M, Brocchi S, Cucchetti A, Mazzotti F, Mosconi C, Sportoletti C, Brandi G, Pinna AD, Golfieri R. Can current preoperative imaging be used to detect microvascular invasion of hepatocellular carcinoma? Radiology 2016; 279: 432-442.

[19] Kim H, Park MS, Choi JY, Park YN, Kim MJ, Kim KS, Choi JS, Han KH, Kim E, Kim KW. Can microvessel invasion of hepatocellular carcinoma be predicted by pre-operative MRI? Eur Radiol 2009; 19: 1744-1751.

[20] Chou CT, Chen RC, Lin WC, Ko CJ, Chen CB, Chen YL. Prediction of microvascular invasion of hepatocellular carcinoma: preoperative CT and histopathologic correlation. AJR Am J Roentgenol 2014; 203: W253-W259.

[21] Chou CT, Chen RC, Lee CW, Ko CJ, Wu HK, Chen YL. Prediction of microvascular invasion of hepatocellular carcinoma by pre-operative CT imaging. Br J Radiol 2012; 85: 778-783.

[22] Kim KA, Kim MJ, Jeon HM, Kim KS, Choi JS, Ahn SH, Cha SJ, Chung YE. Prediction of microvascular invasion of hepatocellular carcinoma: usefulness of peritumoral hypointensity seen on gadoxetate disodium-enhanced hepatobili-

ary phase images. J Magn Reson Imaging 2012; 35: 629-634.
[23] Nagano Y, Shimada H, Takeda K, Ueda M, Matsuo K, Tanaka K, Endo I, Kunisaki C, Togo S. Predictive factors of microvascular invasion in patients with hepatocellular carcinoma larger than 5 cm. World J Surg 2008; 32: 2218-2222.
[24] Hirokawa F, Hayashi M, Miyamoto Y, Asakuma M, Shimizu T, Komeda K, Inoue Y, Uchiyama K. Outcomes and predictors of microvascular invasion of solitary hepatocellular carcinoma. Hepatol Res 2014; 44: 846-853.
[25] Ahn SY, Lee JM, Joo I, Lee ES, Lee SJ, Cheon GJ, Han JK, Choi BI. Prediction of microvascular invasion of hepatocellular carcinoma using gadoxetic acid-enhanced MR and (18)F-FDG PET/CT. Abdom Imaging 2015; 40: 843-851.
[26] Ariizumi S, Kitagawa K, Kotera Y, Takahashi Y, Katagiri S, Kuwatsuru R, Yamamoto M. A non-smooth tumor margin in the hepatobiliary phase of gadoxetic acid disodium (Gd-EOB-DTPA)-enhanced magnetic resonance imaging predicts microscopic portal vein invasion, intrahepatic metastasis, and early recurrence after hepatectomy in patients with hepatocellular carcinoma. J Hepatobiliary Pancreat Sci 2011; 18: 575-585.
[27] Nishie A, Yoshimitsu K, Asayama Y, Irie H, Tajima T, Hirakawa M, Ishigami K, Nakayama T, Kakihara D, Nishihara Y, Taketomi A, Honda H. Radiologic detectability of minute portal venous invasion in hepatocellular carcinoma. AJR Am J Roentgenol 2008; 190: 81-87.
[28] Ros PR, Murphy BJ, Buck JL, Olmedilla G, Goodman Z. Encapsulated hepatocellular carcinoma: radiologic findings and pathologic correlation. Gastrointest Radiol 1990; 15: 233-237.
[29] Grazioli L, Olivetti L, Fugazzola C, Benetti A, Stanga C, Dettori E, Gallo C, Matricardi L, Giacobbe A, Chiesa A. The pseudocapsule in hepatocellular carcinoma: correlation between dynamic MR imaging and pathology. Eur Radiol 1999; 9: 62-67.
[30] Adachi E, Maeda T, Kajiyama K, Kinukawa N, Matsumata T, Sugimachi K, Tsuneyoshi M. Factors correlated with portal venous invasion by hepatocellular carcinoma: univariate and multivariate analyses of 232 resected cases without preoperative treatments. Cancer 1996; 77: 2022-2031.
[31] Lim JH, Choi D, Park CK, Lee WJ, Lim HK. Encapsulated hepatocellular carcinoma: CT-pathologic correlations. Eur Radiol 2006; 16: 2326-2333.
[32] Witjes CD, Willemssen FE, Verheij J, van der Veer SJ, Hansen BE, Verhoef C, de Man RA, Ijzermans JN. Histological differentiation grade and microvascular invasion of hepatocellular carcinoma predicted by dynamic contrast-enhanced MRI. J Magn Reson Imaging 2012; 36: 641-647.
[33] Xu P, Zeng M, Liu K, Shan Y, Xu C, Lin J. Microvascular invasion in small hepatocellular carcinoma: is it predictable with preoperative diffusion-weighted imaging? J Gastroenterol Hepatol 2014; 29: 330-336.
[34] Chandarana H, Robinson E, Hajdu CH, Drozhinin L, Babb JS, Taouli B. Microvascular invasion in hepatocellular carcinoma: is it predictable with pretransplant MRI? AJR Am J Roentgenol 2011; 196: 1083-1089.
[35] Janevska D, Chaloska-Ivanova V, Janevski V. Hepatocellular carcinoma: risk factors, diagnosis and treatment. Open Access Maced J Med Sci 2015; 3: 732-736.
[36] Grandhi MS, Kim AK, Ronnekleiv-Kelly SM, Kamel IR, Ghasebeh MA, Pawlik TM. Hepatocellular carcinoma: from diagnosis to treatment. Surg Oncol 2016; 25: 74-85.